Z6
copies

NASA TECHNICAL MEMORANDUM

NASA TM X-52286

NASA TM X-52286

EXPERIMENTAL STUDIES OF CAVITATION DAMAGE IN ALKALI METAL PUMPS FOR APPLICATION IN SPACE POWER SYSTEMS

by Cavour H. Hauser
Lewis Research Center
Cleveland, Ohio

TECHNICAL PAPER proposed for presentation at Symposium on Testing Techniques in Ship Cavitation Research sponsored by the Norwegian Ship Model Experiment Tank Trondheim, Norway, May 31 - June 2, 1967

NATIONAL AERONAUTICS AND SPACE ADMINISTRATION · WASHINGTON, D.C. · 1967

EXPERIMENTAL STUDIES OF CAVITATION DAMAGE IN ALKALI METAL PUMPS FOR APPLICATION IN SPACE POWER SYSTEMS

by Cavour H. Hauser

Lewis Research Center
Cleveland, Ohio

TECHNICAL PAPER proposed for presentation at

Symposium on Testing Techniques in Ship Cavitation Research
sponsored by the Norwegian Ship Model Experiment Tank
Trondheim, Norway, May 31 - June 2, 1967

NATIONAL AERONAUTICS AND SPACE ADMINISTRATION

EXPERIMENTAL STUDIES OF CAVITATION DAMAGE IN ALKALI METAL PUMPS FOR APPLICATION IN SPACE POWER SYSTEMS

Cavour H. Hauser
National Aeronautics and Space Administration
Lewis Research Center
Cleveland, Ohio, U.S.A.

E-3889

Introduction

To the present time, the relatively modest on-board power requirements for space vehicles in the NASA program have been met primarily through the use of solar cells, chemical batteries and chemical fuel cells. A candidate for large future space electrical power systems is the Rankine cycle turbogenerator system utilizing alkali liquid metal as the working fluid. Such a space power system which would be suitable for power requirements measured in hundreds or even thousands of kilowatts is shown schematically in figure 1. The system would have to be capable of long-term unattended operation with a high degree of reliability.

The heat source for such a system would likely be a nuclear reactor. In the working-fluid loop, sodium or potassium vapor at a temperature of perhaps 2100° F (1422°K) would drive the turbine and be condensed before being pumped back to the boiler. The radiator for rejection of the waste heat is the largest and one of the heaviest components of the system. Because the waste heat must be rejected through radiation to space it is desirable for the radiator to operate at the highest temperature feasible. It is this consideration that suggests the use of one of the alkali metals as the working fluid.

Potassium is the most likely choice although sodium has also been considered. For low radiator weight, subcooling of the condensate should be minimized so that the fluid entering the condensate return pump will be as near to the saturation condition as possible. It would also be desirable, considering system weight, to use a high-speed, high-performance pump. Thus a potential problem in the development of this pump is cavitation and the associated damage. Even if the cavitation damage did not result in structural failure of the impeller, material particles suspended in the working fluid might cause difficulty in other system components, particularly in journal bearings lubricated with the cycle working fluid.

Generally, in the design of pumps, it is desirable to avoid cavitation entirely. If, from considerations of pump weight or cost, this is impractical, suitable materials resistant to cavitation damage are applied, at least in the most critical locations. The properties of the fluid will also affect the damage characteristics of pumps operating with cavitation.

In order to evaluate the severity of cavitation damage in alkali metal pumps and to develop methods for avoiding damage, the Lewis Research Center of NASA has sponsored research in these areas. Studies of cavitation damage in pumps are supplemented by work with the magnetostrictive vibrator. Some of the results to date will be reviewed and summarized.

Tests Using the Magnetostrictive Cavitation Damage Apparatus

In order to determine the relative resistance of a large number of materials in a short time and to make a fundamental study of cavitation damage in liquid metals under carefully controlled conditions the magnetostrictive vibratory device was used in two separate studies. A schematic of the device used at Hydronautics, Inc. (ref. 1) is shown in figure 2. A similar apparatus

was used at the NASA Lewis Research Center (ref. 2).

The apparatus consists of a nickel transducer, an amplifying exponential horn, and an extension-rod specimen holder which cause the specimen to oscillate in a resonant condition when driven by an alternating magnetic field furnished from a power supply. The vibrator apparatus is housed in an argon-filled dry box at atmospheric pressure for all of the tests described herein. Cavitation damage is produced on the surface of the 0.5-inch (1.27cm) diameter specimen which is submerged in the test liquid metal. On each upstroke vapor bubbles are formed near the surface of the specimen. The bubbles collapse with high energy on the ensuing downstroke. Amplitude and frequency are detected with a magnetic pickup. The signal is used in a feedback control circuit providing continuous stable frequency and amplitude output of the apparatus despite variations in resonant frequency induced by temperature changes.

Typical results obtained are shown in figures 3 (ref. 1) and 4 (ref. 2). Rate of volume loss in cubic millimeters per hour is shown as a function of the exposure time in hours. In general the curves are similar in that the damage rate is small initially, rises sharply, and then falls off to a constant steady-state rate. Comparisons among various materials are made in the steady-state zone. The relative damage in 400° F (478°K) sodium for the refractory alloys, TZM, T-222, Cb-132 M, and AISI type 316 stainless steel and Stellite 6B are compared in figure 3. The refractory alloys were chosen because they will maintain a greater strength at the high temperatures of interest in the space power system. At the Lewis Research Center, the iron-base alloys Sicromo 9M, A-286, AISI types 316 and 318 stainless steels, the nickel-base alloys Inconel 600, Hastelloy X, and Rene 41, and cobalt-based alloys L-605 and Stellite 6B were tested in sodium at 800° F (700°K). The results

are compared in figure 4a. In both test series the outstanding resistance to cavitation exhibited by Stellite 6B is evident. The rate curve of cavitation damage for this material for a time duration of ten hours in shown in figure 4b (ref. 3).

In order to determine which physical properties of the material are important in determining the resistance to cavitation damage, it is important to consider the mechanism of damage. Basically, the containment material is exposed to the jet impingement and pressure shock waves of imploding bubbles on or very near its surface. Damage resistance, then, is a measure of the capacity of a material to absorb this mechanical attack before fracture or pitting occurs. Thus, high values of yield strength, ultimate tensile strength, hardness, and ductility (percentage of elongation to fracture) are beneficial in providing resistance to cavitation damage. A. Thiruvengadam has suggested that the cavitation resistance of various materials may be ranked by the strain energy to fracture (ref. 1). Strain energy is the area under the stress-strain curve and may be approximated by the equation

$$\text{Strain Energy} = \frac{(\text{Yield Strength} + \text{Tensile Strength})(\text{Elongation})}{2}$$

The reciprocal of the steady-state volume loss rate in 800° F (700°K) sodium is shown as a function of calculated strain energy for the tests of reference 3 in figure 5. The data points fall close to a straight line with the exception of Stellite 6B which is plotted far above the line. The reason for the outstanding resistance of Stellite 6B is not understood. Possibly the actual strain energy is greater than the calculated value from the approximate equation which assumes a linear stress strain relationship after yield. However, because the damage resistance is so much greater than expected it is likely that properties other than strain energy can control the cavitation

damage resistance of a material. Here, certainly, is an area deserving further study.

The effect of temperature on the rate of cavitation damage for 316 stainless steel immersed in liquid sodium is shown in figure 6 (ref. 1). These results were obtained with the liquid sodium at atmospheric pressure. The damage weight-loss rate is reduced by three orders of magnitude over the range in temperature from 300° to 1500° F, (422° to 1089°K) despite the fact that the specimen material, 316 stainless steel, has less strength at the higher temperature. Similar results were obtained with the refractory materials TZM and T-222 (fig. 7). The reduced damage at high temperature is attributed to changes in the properties of the fluid which cause the cavitation bubbles to collapse with less violence. The effect is further discussed later.

Investigation of Cavitation Damage in an Axial-Flow Pump Stage in Liquid Sodium

Pumps capable of operating with a large amount of cavitation vapor require an axial-flow inlet stage, commonly called an inducer. Such inducer stages are designed for low axial velocity and very high angle of flow with respect to the axial direction at the inlet. Cavitating inducers used in turbopumps for liquid-propellant rocket engines show good performance.

At Lewis Research Center a study was made of the performance and damage characteristics of an axial-flow pump stage with inducer-type blading (ref. 4). The 5-inch (12.70 cm) diameter research rotor having a hub-tip radius ratio of 0.77 is shown in figure 8. Pump overall performance was obtained in liquid sodium for both cavitating and non-cavitating conditions. In addition, a high-temperature cavitation-endurance test in liquid sodium was conducted with insertable blading of three different materials. Because the purpose of the in-

ducer is to raise the pressure sufficiently to suppress cavitation in a following stage having high pressure rise, the inducer has a relatively modest head requirement. For example, at 3450 rpm, and a flow of 240 gpm (0.0151 m^3/sec), a non-cavitating head rise of 24 feet (7.3m) was measured.

An identical rotor, except for direction of rotation, was tested in a water facility with a transparent window in the housing in order to observe the cavitation patterns. The cavitation formations for the operating point corresponding to the endurance run in sodium are shown in figure 9.

Cavitation is present in two separate areas, on the blade suction surface near the leading edge, and in a tip vortex which is generated in the region of interaction between the main-stream through-flow and the secondary blade tip clearance flow from the pressure to the suction surface of the blade. Damage in inducers is usually observed on the blade pressure surface in the region of collapse of the tip clearance vortex from the adjacent blade. Notice in figure 9 that for the relatively short chord blades of this study, the tip vortex cavitation vapor seems to be confined largely to the mid-channel region and is dissipated downstream of the blade row.

The liquid sodium pump test facility is illustrated in figure 10. The pump and volute collector were submerged in the expansion tank as shown in the inset. In this way a rotating liquid sodium shaft seal was unnecessary. The flow from the pump passes through sections of the 4-inch (10 cm) Inconel main line which are heated or cooled for temperature control, a Venturi flowmeter, and throttle valve. Bypass loops are utilized to trap the oxides of sodium that are present and to monitor the sodium oxide concentration. Three blades, each of 316 and 318 stainless steel and Rene 41, were selected for an evaluation of their relative resistance to damage.

The 200-hour cavitation endurance test was conducted at a temperature of 1509° F (1094°K). The speed was 3442 rpm; flow rate, 264 gpm (0.0167 m^3/sec); total head rise, 19.5 feet (6.0 m); and margin of inlet head above vapor head, 17.6 feet (5.4m). This operating point was selected to give a 4 percent drop-off from the non-cavitating head rise and corresponds to the flow condition shown in figure 9.

Post-test examination of the blades indicated that the only significant cavitation damage occurred in a small area on the suction surface near the leading edge and tip of the blade (fig. 11). The photographs also show a roughening of the overall blade surface which was due to corrosion. The white areas in the photographs are residual sodium oxide. As predicted from the magnetostrictive device test results, Rene 41 is the most resistant of the three materials tested.

It is significant that in these tests cavitation damage of the blade pressure surface is negligible. Apparently the tip vortex was confined to the mid-channel region as discussed previously and did not cause damage to the adjacent blade.

Investigation of Cavitation Damage in a Mixed-Flow Impeller in Liquid Potassium

An investigation of cavitation damage in a mixed-flow impeller pumping liquid potassium at 1400° F (1033°K) was made by the Pratt and Whitney Aircraft Division of the United Aircraft Corporation under contract to NASA (ref. 5). The objective was to determine the severity of cavitation damage to the impeller in a controlled endurance run under conditions of rather extensive cavitation. The cast AISI type 316 stainless steel impeller is shown in figure 12. The condition of the impeller blade surfaces was carefully examined before and after the endurance test.

The impeller was tested in both water and potassium. For the endurance run condition, the rotative speed was 6375 rpm; flow, 700 gpm (0.0442 m^3/sec); the head rise about 200 feet (61m); and the net positive suction head, 17.7 feet (5.4m). The cavitation formations in water at this operating point are shown in figure 13. The photograph shows two distinctly separate regions of cavitation. In the entrance region there is a cavity on the suction surface and extensive tip vortex cavitation extending well into the blade passage. A separate tip vortex cavitation pattern exists in the rear channel portion of the blade. This second tip vortex cavitation region results from high blade loading over the rear portion of the blade. The high loading in this region can be inferred from the measured pressure distribution shown in figure 14. Static pressure along the shroud is plotted as a function of the percent axial distance through the pump. The pressure rise is markedly steeper in the downstream portion of the channel. It would be possible to design a similar impeller with reduced loading over the rear portion of the blades so that tip clearance cavitation would be avoided or greatly reduced in this region.

The endurance test of the impeller in potassium was terminated after 350 hours by excessive vibration and mechanical failure of the running gear. Post-test examination of the impeller indicated that there had been an interference between the blade tips and the casing. However, the rotor was intact and the duration of the endurance test was sufficient for an evaluation of of cavitation damage. There was negligible damage over the entrance region of the blades. Only a few small scattered pits were observed on the suction surface of the blades (fig. 15). However, severe cavitation damage did occur on the pressure surfaces of the blades in the region just downstream of the tip clearance cavitation pattern observed in the rear-channel of the blades

(fig. 16). In the most severe damage region, the maximum depth of penetration was 0.050 inch (1.27mm).

The degree of damage varied for the three blades. This variation was related to blade tip clearance, which was different for the three blades because the impeller rotated with a slight eccentricity. The least damage corresponded to the smallest tip clearance.

The marked difference in damage between the inlet and the rear channel portion of the blades can be attributed to the different pressure level in these locations. It is reasonable that the intensity of bubble collapse, and, therefore, damage will increase with a greater difference between the local pressure and vapor pressure in the cavitation region. The effect is discussed in the following section.

The fact that the damage in the pump entrance region was negligible indicates that some cavitation may be tolerable. Although the operating range of a pump designed to operate with cavitation would be limited, in some applications, as in the condensate pump considered in this paper, this might be quite satisfactory.

Effect of Fluid Properties on Cavitation Damage

A fundamental analysis of the mechanics of vapor bubble collapse is presented in reference 6. A parameter, B_{eff}, is derived which can be used to define the mode of collapse of a vapor bubble. It is shown that for $B_{eff} > 10$, the rate of bubble collapse is primarily controlled by the inertia of the liquid. For $B_{eff} < 0.05$ the bubble collapse is much slower and is controlled by the rate at which heat from the condensing vapor in the bubble can be conducted into the surrounding liquid. In the intermediate range, $(0.05 \leq B \leq 10)$ it is indicated that both heat transfer effects and inertia effects will affect the

rate of bubble collapse. Cavitation damage, of course, should be greater in the regime of inertia-controlled bubble collapse.

In reference 7, Garcia derives a modified equation for the evaluation of B_{eff}, which is referred to herein as B^*_{eff},

$$B^*_{eff} = \frac{1}{3600\sqrt{g}}\left[\left(\frac{\rho_L^2\, C_L}{\rho_V L}\right)\left(\frac{\Delta T}{\Delta P}\right)\right]^2 \frac{K_L}{R_o}\,(H\text{-}Hv)^{3/2}$$

where B^*_{eff} thermodynamic bubble parameter, as defined in reference 7, dimensionless

ρ_L liquid density, lb/ft^3

ρ_V vapor density, lb/ft^3

C_L liquid specific heat, $Btu/lb\,^oF$

L latent heat, Btu/lb

$\frac{\Delta T}{\Delta P}$ reciprocal slope of vapor pressure curve, $^oF/(lb/ft^2)$

K_L thermal diffusivity, ft^2/hr

R_o characteristic bubble radius, ft

$H\text{-}Hv$ margin of static head above vapor pressure head, ft

g acceleration of gravity, ft/sec^2

It is difficult to compute meaningful absolute values for B^*_{eff} for actual conditions in a pump or for a magnetostrictive-device experiment because the effective values of bubble radius and local value of (H-Hv) can only be estimated. Examination of the equation for B^*_{eff} however, gives insight into the thermal fluid properties affecting bubble collapse rate. In general, if arbitrary values are assigned for R_o and ambient

head, H, the calculated value of B^*_{eff} is reduced markedly at higher temperatures, primarily because of changes in the values of vapor density, ρ_v, and the ratio, $(\Delta T/\Delta P)$. If atmospheric ambient pressure is assumed, B^*_{eff} for sodium is lower by eight orders of magnitude between 900° F (756° K) and 1500° F (1089° K). It is suggested in reference 7 that these thermal effects can account for the sharp drop in cavitation damage rates at high temperature in the magnetostrictive device tests (figs. 6 and 7). At lower temperatures corresponding to very high values of B^*_{eff} (400° - 700° F) (478° - 644° K) it seems clear that bubble collapse time is inertia controlled. The marked decrease in damage rate at the higher temperatures, particularly at 1500° F (1089° K) can be attributed to a lower intensity bubble collapse caused by a heat-transfer-controlled collapse rate. Cavitation damage on the blading of the axial-flow rotor run in sodium at 1509° F (1094° K) might have been more severe except for these fluid property effects.

These considerations also offer an explanation for the different damage rates for the entrance region and the rear-channel portion of the mixed-flow impeller run in 1400° F (1033° K) liquid potassium. If B^*_{eff} is evaluated using the local static pressure to calculate $(H-H_v)$, the value in the rear channel, where cavitation damage is severe, is about ten times greater than in the entrance region. This could well account for the difference in damage.

It should be emphasized that the parameter, B^*_{eff}, is only a measure of the relative inertia and heat transfer effects on the rate of bubble collapse. Other factors important in controlling damage such as the quantity of dissolved gas in the liquid, the effect of fluid density or pressure in inertia-controlled collapse, surface tension, viscosity, and sonic velocity in the liquid are not considered. The total effect of the fluid physical and thermodynamic properties on cavitation damage are not adequately understood.

Summary Remarks

Some of the results of this research program on cavitation damage in alkali metal pumps are summarized.

The relative damage resistance of a number of materials has been evaluated and some insight on the material properties controlling damage has been obtained.

Experimental studies of pumps have suggested two ways in which damage can be controlled. In an axial-flow stage damage from tip clearance cavitation in sodium at 1509° F (1094° K) was avoided because in these short chord blades this cavitation formation was confined to the midchannel region and did not collapse on the blade surface. Cavitation damage in the relatively low-pressure entrance region of a mixed-flow impeller pumping liquid potassium at 1400° F (1033° K) was negligible because the physical properties of the fluid in this region caused the vapor bubbles to collapse with less violence. Cavitation in the high pressure region of this impeller caused severe damage.

When this program was initiated it was generally considered that cavitation damage in alkali metal pumps would pose a severe design problem. Overall, the results obtained to date are encouraging; it should be possible to design relatively lightweight pumps for application in space power systems.

REFERENCES

1. Thiruvengadam, A.; and Preiser, H. S.: Cavitation Damage in Liquid Metals. Rep. No. TR-467 (NASA CR-72035), Hydronautics, Inc., Nov. 29, 1965.

2. Young, Stanley G.; and Johnston, James R.: Accelerated Cavitation Damage of Steels and Superalloys in Liquid Metals. NASA TN D-3426, 1966.

3. Young, Stanley G.; and Johnston, James R.: Accelerated Cavitation Damage of Steels and Superalloys in Sodium and Mercury. Paper presented at the 69th Annual Meeting of the ASTM, Atlantic City, June 26 - July 1, 1966.

4. Reemsnyder, Dean C.; Cunnan, Walter S.; and Weigel, Carl: Investigation of Performance and Cavitation Damage of an Axial-Flow Pump in High Temperature Sodium. Proposed NASA Technical Note.

5. Kulp, Robert S.; and Altieri, James V.: Cavitation Damage of Mechanical Pump Impellers Operating in Liquid Metal Space Power Loops. Pratt and Whitney Aircraft (NASA CR-165), July 1965.

6. Florschuetz, L. W.; and Chao, B. T.: On the Mechanics of Vapor Bubble Collapse. J. Heat Transfer, vol. 87, no. 2, May 1965, pp. 209-220.

7. Garcia, Ramon: Comprehensive Cavitation Damage Data for Water and Various Liquid Metals Including Correlations with Material and Fluid Properties. Rep. No. 05031-6-T, University of Michigan, Aug. 1966.

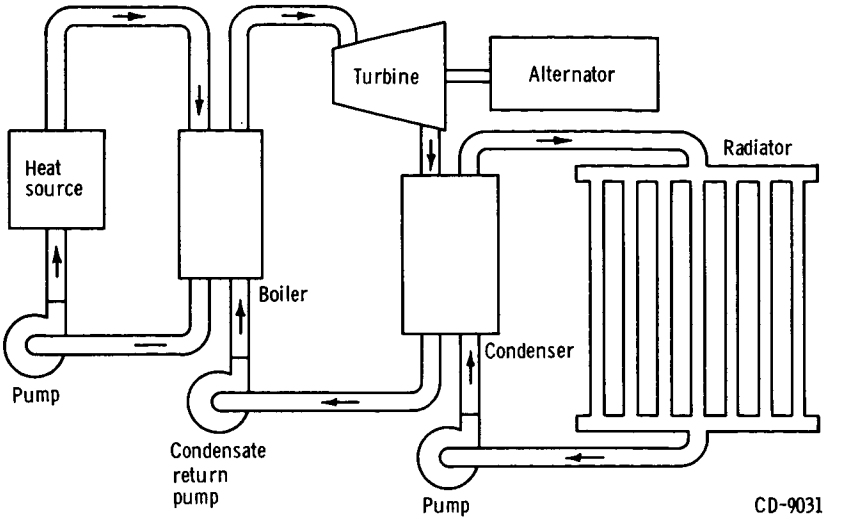

Figure 1. - Turbogenerator space power system.

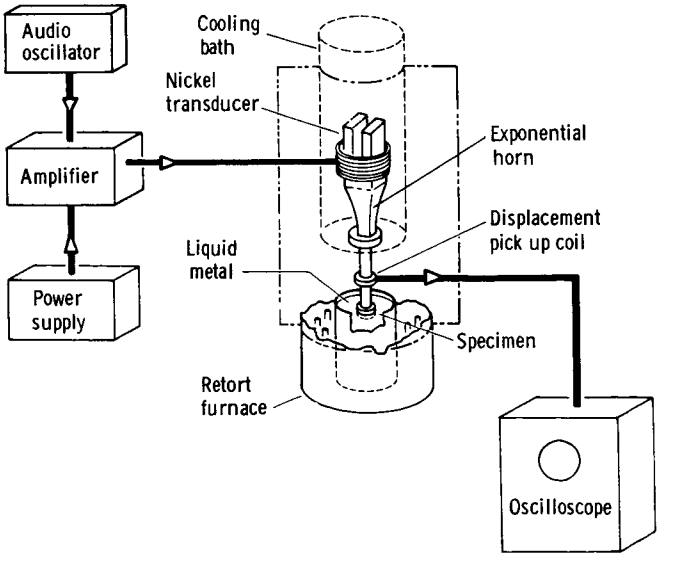

Figure 2. - Block diagram of the magnetostrictive apparatus used for cavitation damage tests.

E-3889

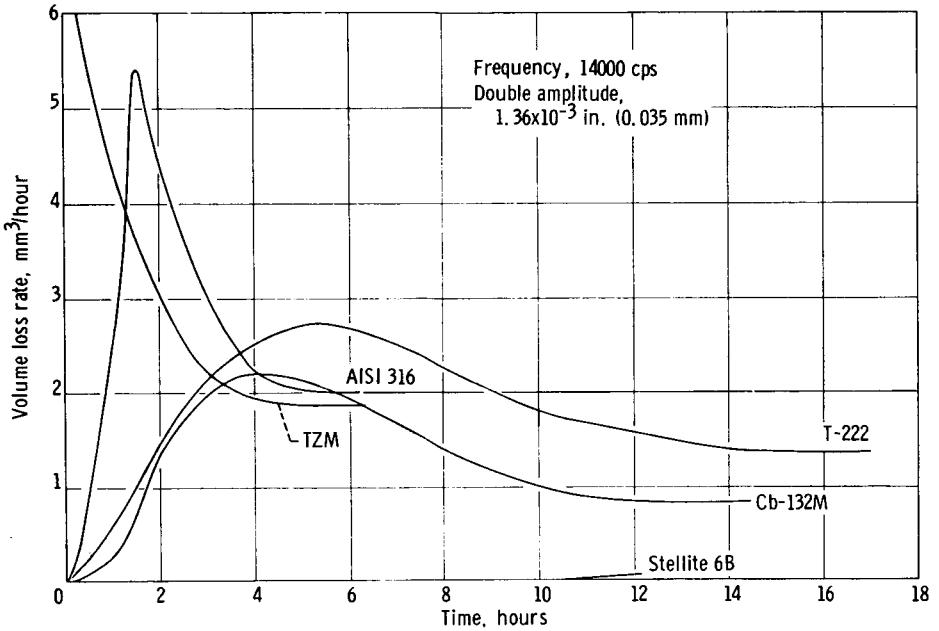

Figure 3. - Volume loss rate for five metals tested in 400° F (478° K) sodium.

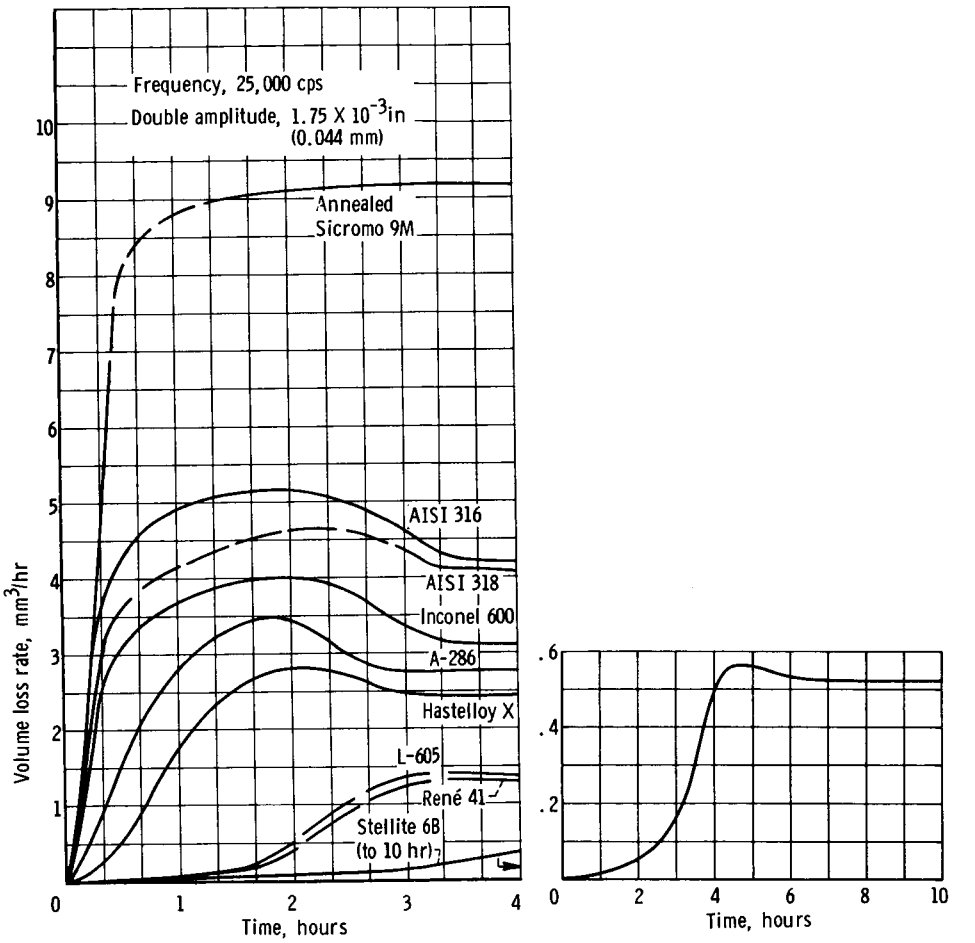

(a) Various materials.

(b) Stellite 6B.

Figure 4. - Rate of cavitation damage of materials in sodium at 800° F (700° K).

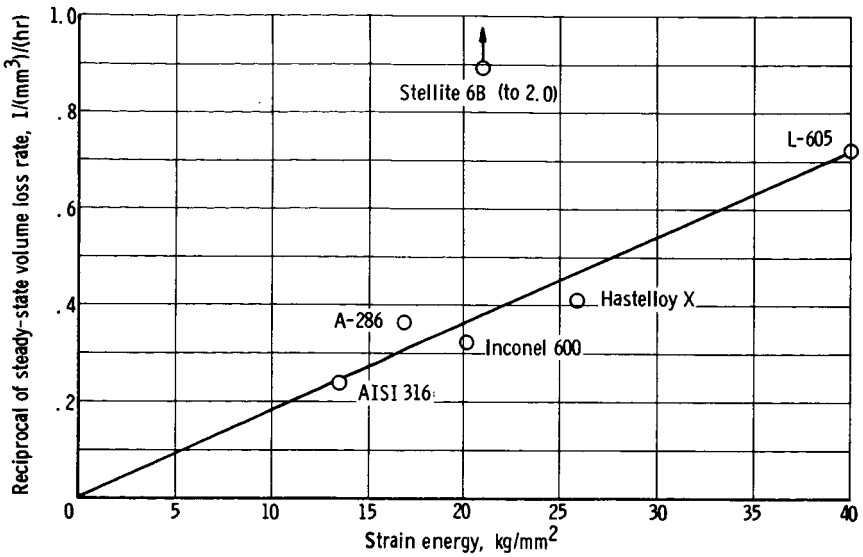

Figure 5. - Relation of cavitation damage in sodium at 800° F (700° K) with strain energy parameter.

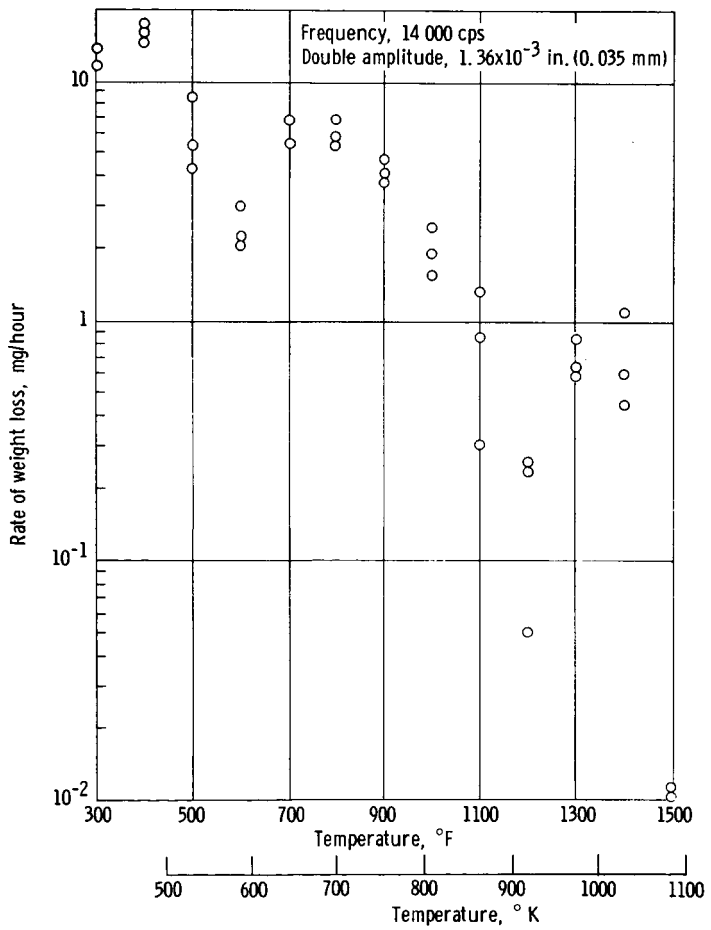

Figure 6. - Effect of temperature on the cavitation damage rate in magnetostrictive device for AISI 316 stainless steel in liquid sodium.

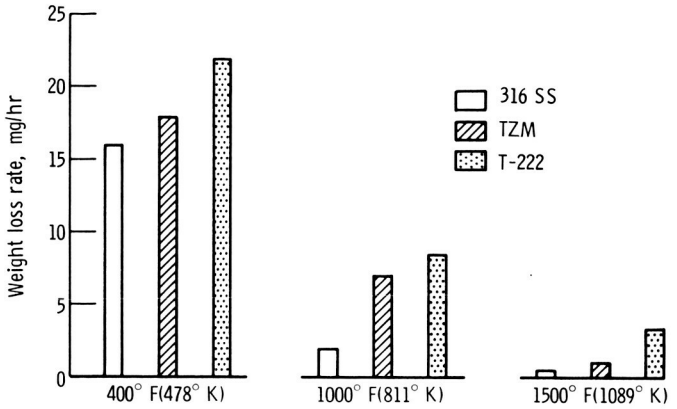

Figure 7. - Effect of temperature on cavitation damage rate in magnetostrictive device in liquid sodium.

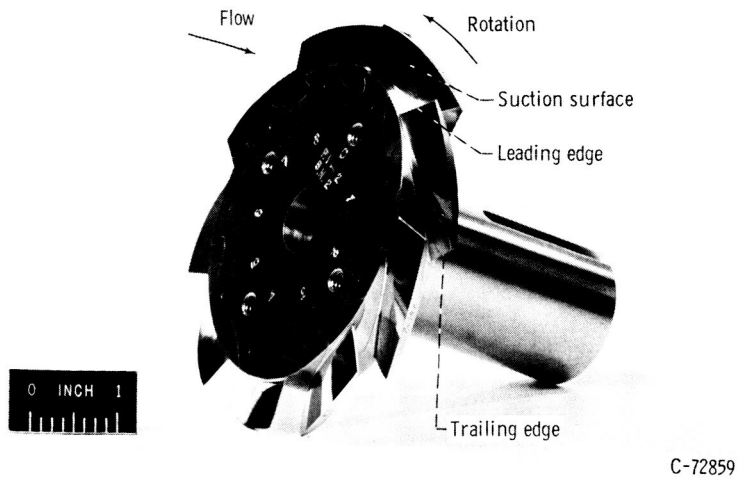

Figure 8. - Axial-flow rotor for sodium tests.

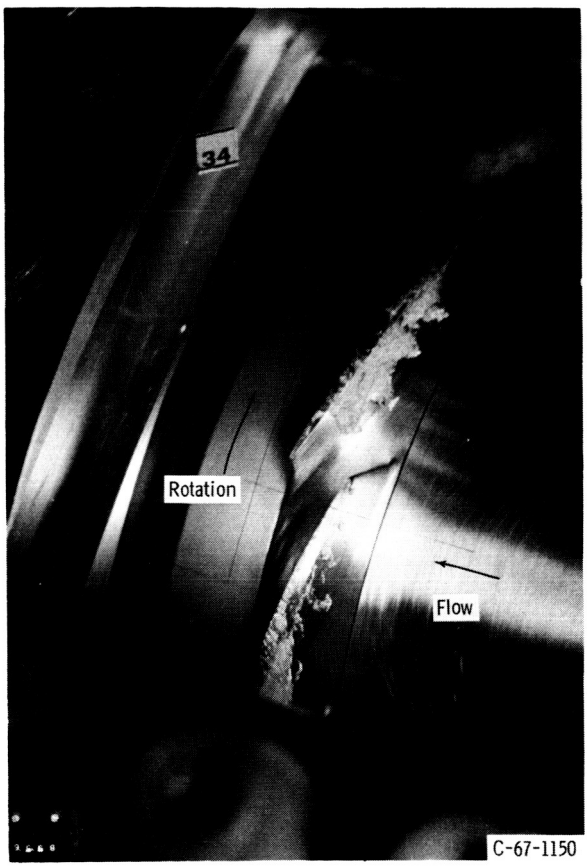

Figure 9. - Axial-flow rotor - cavitation formation in water at 80° F (300° K).

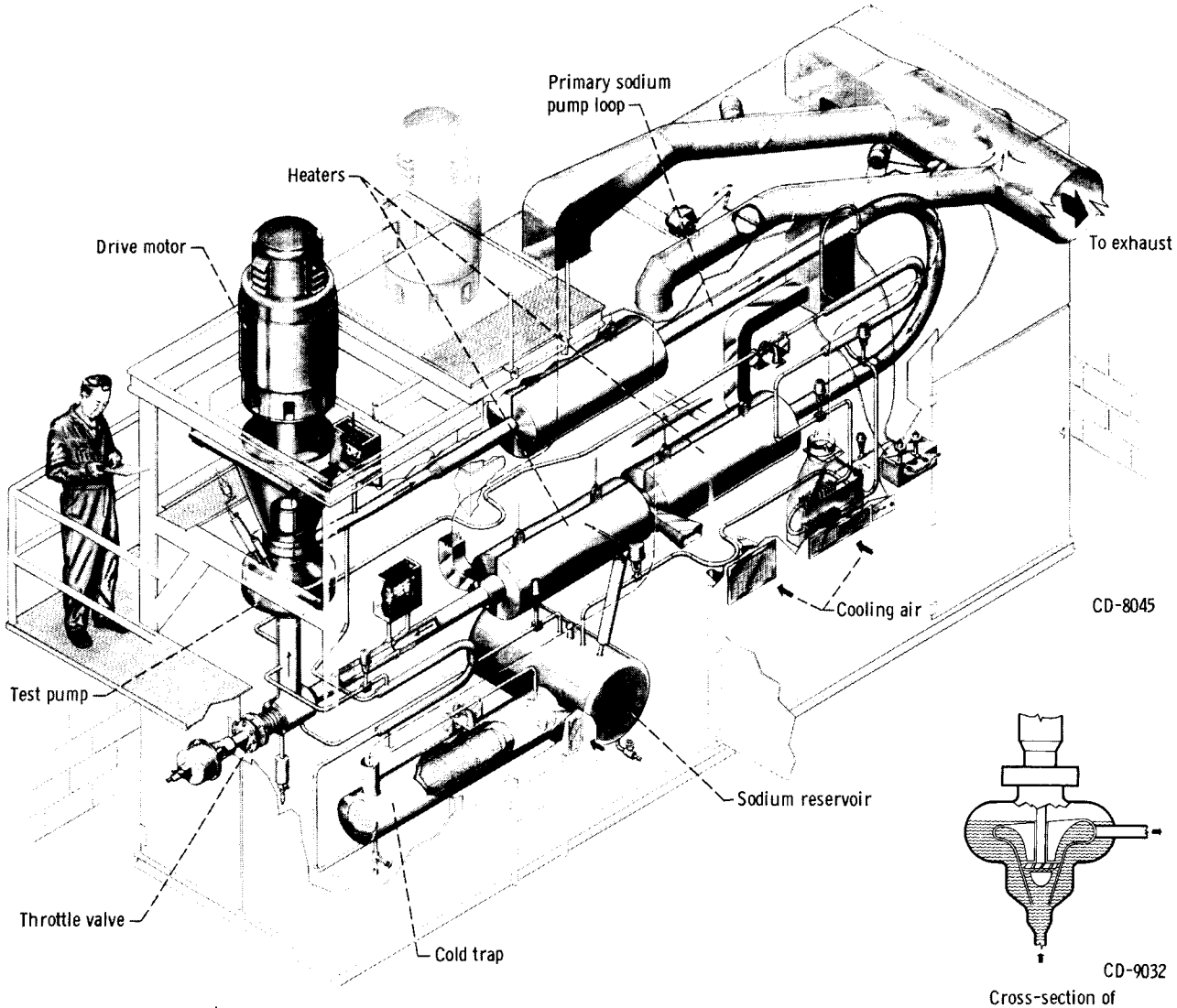

Figure 10. - Sodium pump test facility.

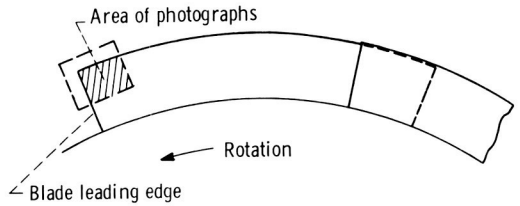

Location of damage

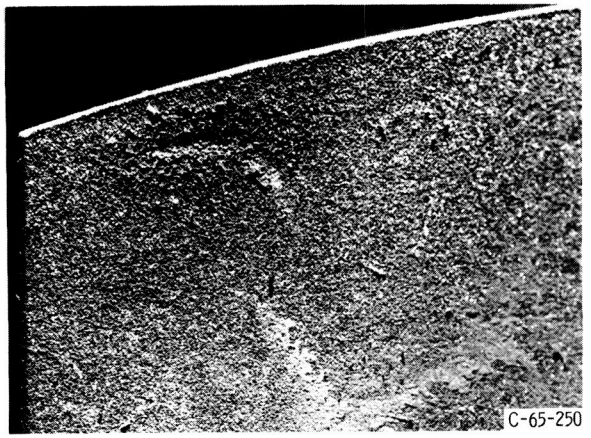

AISI 316 stainless steel

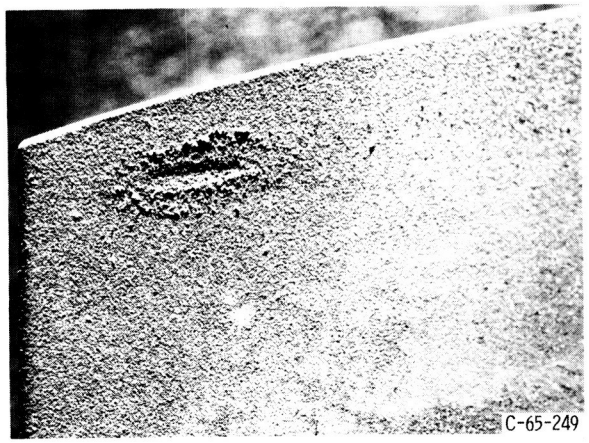

AISI 318 stainless steel

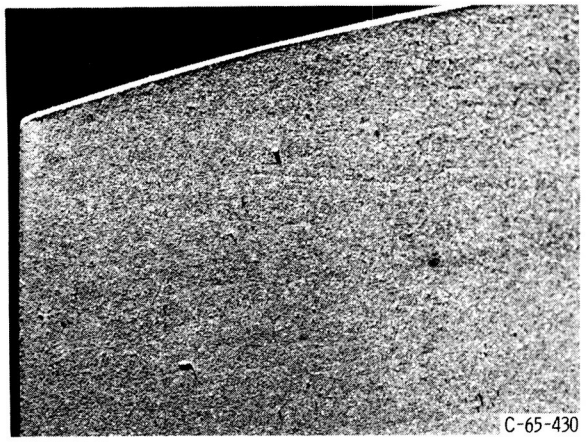

Rene 41

Figure 11. - Cavitation damage to pump impeller blades of three different materials operated in liquid sodium for 200 hours at 1500° F (1090° K).

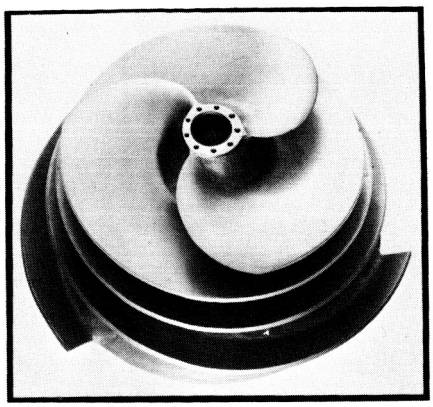

C-67-1106

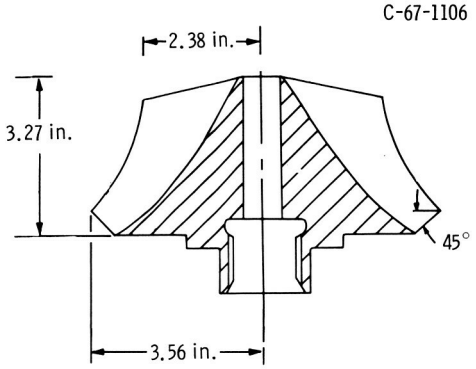

Figure 12. - Mixed-flow impeller for potassium tests.

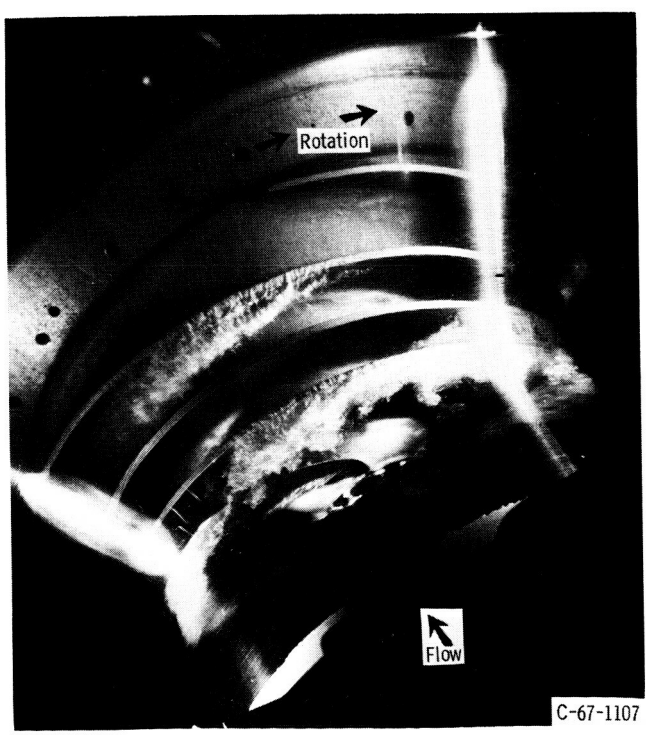

Figure 13. - Mixed-flow impeller - cavitation formation in water at 80° F (300° K).

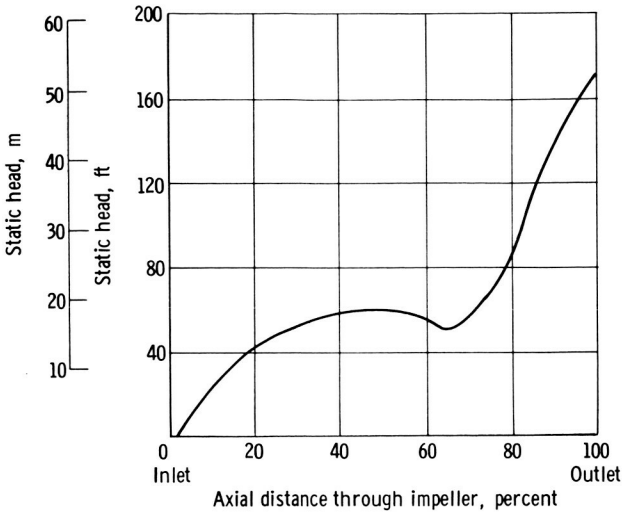

Figure 14. - Mixed-flow impeller tip static head distribution.

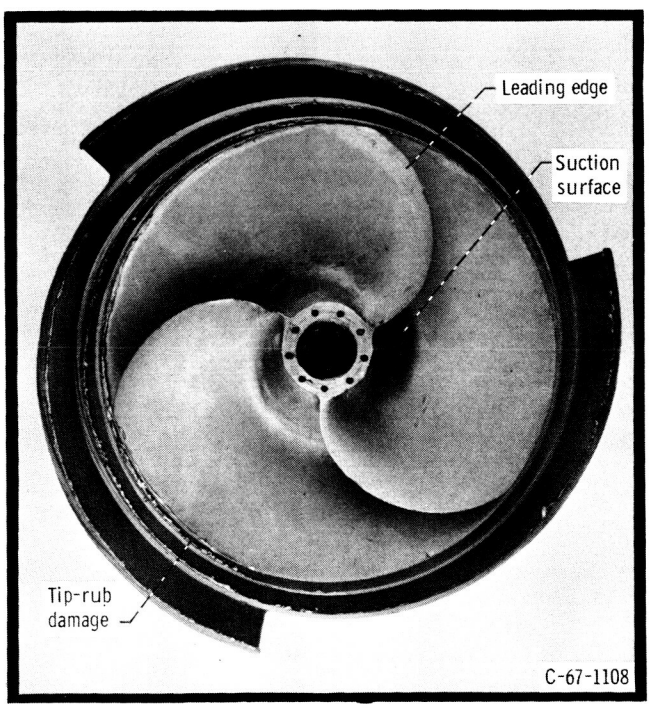

Figure 15. - Mixed-flow impeller after potassium tests.

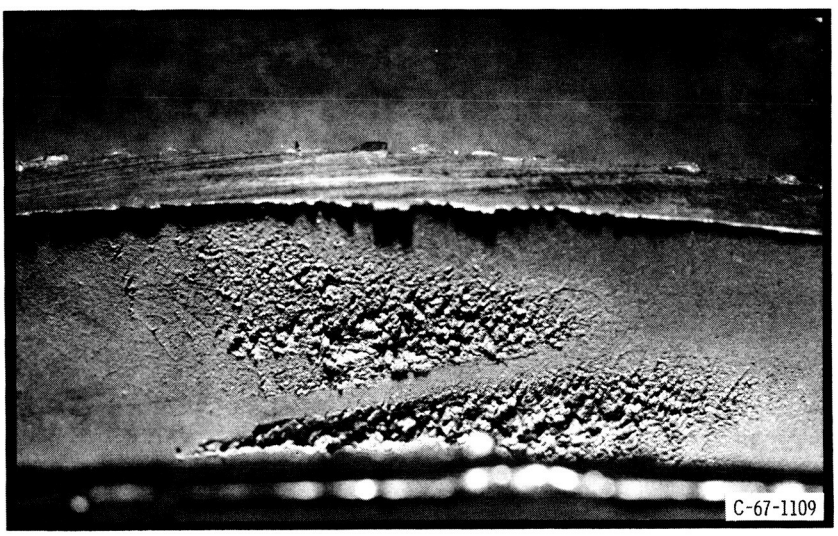

Figure 16. - Cavitation damage on rear channel pressure surface of mixed-flow impeller.